

# Jamming of frictional spheres and random loose packing

Leonardo E. Silbert\*

*Department of Physics, Southern Illinois University, Carbondale, IL, USA.*

The role of friction coefficient,  $\mu$ , on the jamming properties of disordered, particle packings is studied using computer simulations. Compressed, soft-sphere packings are brought towards the jamming transition - the point where a packing loses mechanical stability - by decreasing the packing fraction. The values of the packing fraction at the jamming transition,  $\phi_c^\mu$ , gradually decrease from the random close packing point for zero friction, to a value coincident with random loose packing as the friction coefficient is increased over several orders of magnitude. This is accompanied by a decrease in the coordination number at the jamming transition,  $z_c^\mu$ , which varies from approximately six to four with increasing friction. Universal power law scaling is observed in the pressure and coordination number as a function of distance from the generalised, friction-dependent jamming point. Various power laws are also reported between the  $\phi_c^\mu$ ,  $z_c^\mu$ , and  $\mu$ . Dependence on preparation history of the packings is also investigated.

PACS numbers: 45.70.-n 83.80.Fg 61.43.-j 64.70.ps

## Introduction

Granular packings can exist over a range of densities generally depending on the generation protocol and the nature of the grain-grain interactions. For *frictionless* spheres, where the particle friction coefficient  $\mu = 0$ , *random close packing* (rcp), or the maximally random jammed state, describes the densest possible packing of dry, cohesionless, spheres whose structure contains no long-range order [1–8]. Random close packing is well-defined in the sense that it represents a reproducible packing state as observed in numerous experiments and simulations of frictionless sphere packings of hard particles that interact primarily through excluded volume effects [9]. All such studies agree that random close packing occurs at a packing fraction,  $\phi_{\text{rcp}} \approx 0.64$ . This is in contrast to *frictional* packings,  $\mu > 0$ , which can exist over a substantial range in packing fraction from  $\phi_{\text{rcp}}$  all the way down to  $\phi_{\text{rlp}} \approx 0.55$ , the value often quoted as *random loose packing* [10, 11]. Although, in reality, it is actually quite difficult to generate loose packed states. Consequently, random loose packing is a much less well-developed concept than random close packing. The strong history dependence and characterisation of frictional packings persists as an experimental issue thus opening the door for simulations to shed light on the nature of random loose packing of frictional particles.

Frictionless sphere-packings and the rcp state have received much focus in terms of *jamming* - the transition from a jammed, rigid, solid-like state, with finite shear and bulk moduli, to an unjammed, liquid-like state [6, 12–14]. The simplest system exhibiting such a transition occurs in a packing of over-compressed, purely-repulsive, soft, frictionless spheres, at zero temperature in the absence of gravity. As the packing fraction,  $\phi$ , is decreased, the packing undergoes a transition

at  $\phi_c$ , between jammed and unjammed phases that occurs abruptly at  $\phi_c = \phi_{\text{rcp}}$ . Approaching the jamming transition from above,  $\phi \rightarrow \phi_c^+$ , the average number of contacting neighbours per particle - the coordination number  $z$  - approaches the minimal value required for mechanical stability  $z_{\text{iso}}$ , also known as isostaticity. For frictionless spheres,  $z_{\text{iso}}^{\mu=0} = 6$  (in  $3D$ ,  $= 4$  in  $2D$ ) [15–17]. Thus, the interplay between mechanical stability and maximally random [4], in some sense, provides a meaningful operational definition of the rcp state. Although it is worthwhile to note that the particle positions are disordered - no long range order exists - but they are not completely random as they must satisfy mechanical equilibrium.

The question now arises, to what extent do these developing ideas of jamming apply more generally in systems with non-central force laws, such as frictional, granular packings? The identification of the jamming threshold in frictionless sphere packings to the well-known rcp state begs the question, can these same ideas lead to a more concrete definition of the random loose packing state for frictional spheres? These concerns are investigated here by studying how interparticle friction affects the jamming properties of monodisperse spheres. Here it is shown that the extrapolated values of the packing fraction  $\phi_c^\mu$ , and the coordination number  $z_c^\mu$ , at the jamming transition depend on the friction coefficient  $\mu$ , as presented in I and 1, in agreement with conclusions of recent experiments [11] and theory [5, 18–22], and that  $\phi_c \rightarrow \phi_{\text{rlp}}$  and  $z_c \rightarrow z_{\text{iso}}^{\mu=\infty} = 4$  (in  $3D$ ,  $= 3$  in  $2D$ ) in the limit of large friction. Here,  $z_{\text{iso}}^{\mu=\infty}$  represents the isostatic state for frictional spheres, corresponding to the minimally required coordination number for infinitely hard, frictional spheres [23]. Although the main focus of this study is three dimensional packings, for completeness, some information for  $2D$  packings is also provided in 1 and I.

To date, the influence of friction has been studied in the context of three dimensional granular packings [18, 24–26], and, to some extent, their jamming prop-

---

\*lsilbert@physics.siu.edu

TABLE I: Extrapolated values of the packing fraction  $\phi_c^\mu$ , and coordination number  $z_c^\mu$ , at the jamming transition for different friction coefficient  $\mu$  for 3D monodisperse spheres (top) and 2D bidisperse discs (bottom). The associated errors on these estimates range from less than 1% for small  $\mu$  to 4% at larger values of  $\mu$ .

3D								
$\mu$	0	0.001	0.01	0.1	0.2	0.5	1	10
$\phi_c^\mu$	0.639	0.638	0.634	0.614	0.595	0.574	0.556	0.544
$z_c^\mu$	5.96	5.93	5.76	5.17	4.60	4.22	3.98	3.88

2D								
$\mu$	0	0.001	0.01	0.1	0.2	0.5	1	10
$\phi_c^\mu$	0.843	0.843	0.842	0.836	0.827	0.801	0.779	0.767
$z_c^\mu$	3.96	3.86	3.85	3.73	3.59	3.15	2.91	2.97

erties [5, 19, 22]. Makse and co-workers [22] recently made significant contributions to our understanding of frictional packings from a theoretical point of view and the results presented here are fully consistent with these previous studies. In saying that, however, most earlier studies have not accurately addressed the issue as to whether frictional packings jam in the same way as frictionless ones nor has the issue of history dependence been seriously considered. These are the two principal themes investigated in this study.

What is apparent is that the computational models employed are fully relevant to address realistic systems. In particular, experiments [27, 28] and simulations [21, 29, 30] of pseudo-2D, jammed, disc packings show good agreement suggesting that the phenomenon of jamming seems to be applicable to real, frictional materials. Here, it is shown that friction does indeed play an essential role in determining the jamming transition for 3D sphere-packings as is the case in two dimensional simulations of the Leiden group [21, 30]. The principal result is the contention that the concept of the random loose packing state becomes a friction-dependent property. The commonly quoted value for  $\phi_{\text{rlp}} \approx 0.55$ , is only realised in the limit of large friction. Moreover, power law scaling is observed in the pressure and excess coordination relative to the friction-dependent jamming transition and that these critical values also exhibit power law behaviour with friction coefficient.

### Simulation Model

The simulation technique used here employs  $N = 1024$  monodisperse, inelastic, soft-spheres of diameter  $d = 1$  and mass  $m = 1$ , within a cubic simulation box with periodic boundary conditions without gravity. Particles interact only on contact when they overlap, at which point they are considered to be contacting neighbours, through a repulsive, linear spring-dashpot. The repulsive force is

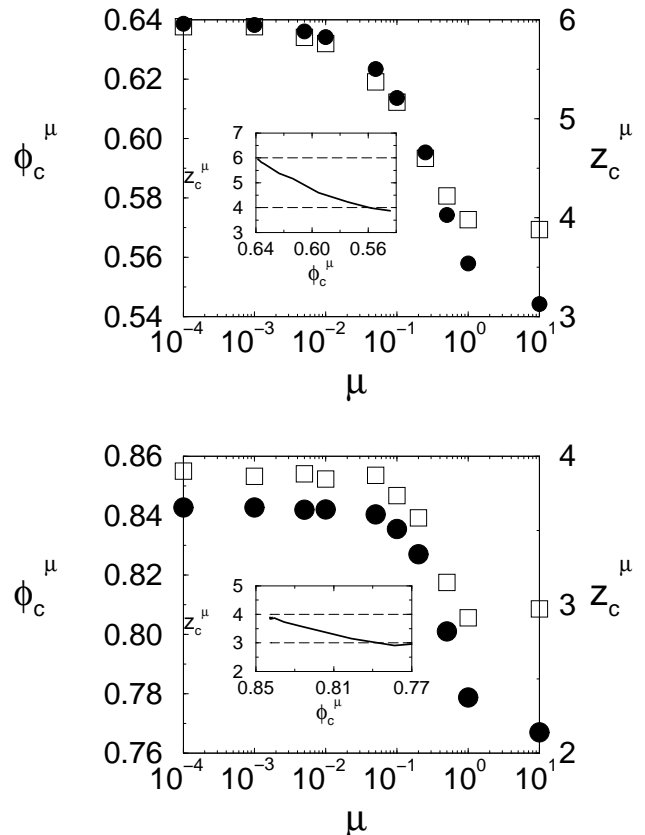


FIG. 1: Dependence of the critical values of the packing fraction  $\phi_c^\mu$  (filled circles), and coordination number  $z_c^\mu$  (open squares), on the particle friction coefficient  $\mu$ , for monodisperse spheres in 3D (upper panel) and bidisperse discs in 2D (lower panel). The insets are parametric plots of  $\phi_c^\mu$  against  $z_c^\mu$ . Symbol size is representative of sample-to-sample fluctuations and error bars.

characterised by the particle stiffness  $k_{n,t}$ , and inelasticity by the coefficient of restitution  $e_{n,t}$ , in the normal ( $n$ ) and tangential ( $t$ ) directions with respect to the contact surfaces. Unless otherwise stated, for  $\mu > 0$ , a static friction law tracks the history of the friction forces over the lifetime of a contact that satisfies the Coulomb yield criterion [18, 31–33]. In this work, the particle Poisson ratio,  $\nu = \frac{1-\lambda}{4+\lambda} = 0$  [34], where the ratio of the tangential to the normal particle stiffness is denoted by,  $\lambda \equiv \frac{k_t}{k_n} = 1$ , for this study.

The initial configurations were generated by taking a dilute assembly of particles in a disordered, liquid-like configuration, then instantaneously quenching these configurations into over-compressed, jammed packed states at  $\phi_i = 0.65$ . After this rapid compression the configurations were then allowed to relax into a mechanically stable state. Unless otherwise stated, during this initial compression friction was switched off. In an alternative protocol to be discussed later, friction was switched on during the initial quench to the over-compressed state.

The packing fraction of these mechanically stable packings were then incrementally decreased towards the jamming threshold with the friction coefficient set at the desired value. After each incremental change in the packing fraction, the packing was rapidly quenched back into a mechanically stable state by setting  $e_{n,t} \approx 0$ . This procedure was continued until the difference in the potential energy between successive increments  $\lesssim 10^{-16}$ , at which point the simulation run terminates. To improve statistical uncertainty, all results are averaged over at least five independent realisations.

## Results and discussion

The jamming transition is identified as the point at which the pressure  $p$ , computed from the contact stresses, goes to zero. The jamming transition packing fraction  $\phi_c$ , is obtained as a fitting parameter by extrapolating the  $\phi - p$  curve to  $p = 0$ . Likewise, the coordination number at the transition,  $z_c$ , is similarly obtained by fitting the  $(p, z)$  data to the functional form used for frictionless spheres [14] and bubbles [35]:  $p \propto (z - z_c)^{1/2}$ . This same power law exponent has also been used to fit experimental [28] and numerical data [19, 21] of frictional systems.

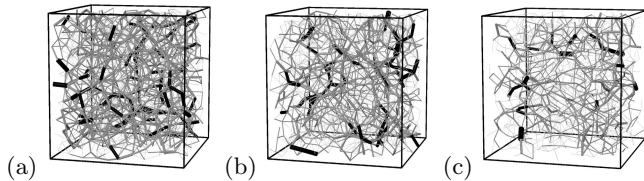


FIG. 2: Snapshots of the normal force networks for three different friction coefficients at approximately the same pressures or equivalently the same  $\Delta\phi^\mu \approx 10^{-4}$ ; (a)  $\mu = 0$ , (b)  $\mu = 0.1$ , and (c)  $\mu = 1$ . Lines represent the normal forces between particles in contact. Thicker, darker lines indicate larger forces. Particles not shown for clarity.

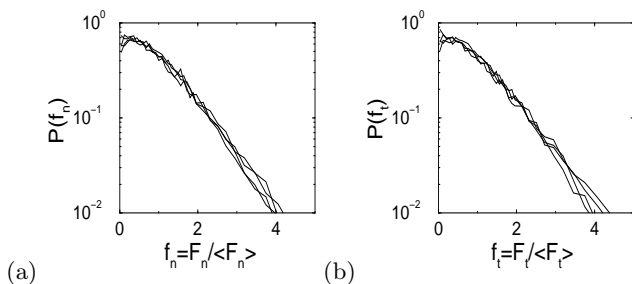


FIG. 3: Distributions,  $P(f_{n,t})$ , of the, (a) normal  $F_n$ , and (b) tangential  $F_t$ , contact forces, normalised by their respective mean values. Data at approximately the same  $\Delta\phi^\mu \approx 10^{-4}$  for four different friction coefficients are shown:  $\mu = 0.001, 0.1, 0.25, 1$ . The data at  $\mu = 0.25$  is emphasised.

The transition values,  $\phi_c^\mu$  and  $z_c^\mu$ , for different  $\mu$ , are shown in I and plotted in 1. The insets in 1 represent the

boundary between stable and unstable states. For 3D, monodisperse spheres with  $\mu = 0$ ,  $\phi_c^{\mu=0} = 0.64 \pm 0.001$  and  $z_c^{\mu=0} = 5.96 \pm 0.05$ , are indistinguishable from previous studies that used similar and different algorithms [7, 14, 18, 19, 36]. These results are consistent with  $\phi_{rcp}$  and  $z_{iso}^{\mu=0}$ . As  $\mu$  increases,  $\{\phi_c^\mu, z_c^\mu\}$  decrease. In the limit of large friction,  $\mu \geq 1$ , these values saturate at about,  $\phi_c^{\mu=\infty} \approx 0.55$  and  $z_c^{\mu=\infty} \approx 4$ , which coincide with the values of  $\phi_{rlp}$  and  $z_{iso}^{\mu=\infty}$ . To check that these values do indeed correspond to the hard-particle limit, the particle stiffnesses were varied over five orders of magnitude keeping their ratio  $\lambda = 1$ . The resulting critical values obtained were all indistinguishable within statistical error. For completeness data for two dimensional, bidisperse disc packings (with particle size ratio 1:1.4) is also shown in 1 and I. The 2D data are consistent with other jamming results [21], simulations of sheared granular materials [37], and studies on force indeterminacy [20].

This behaviour can be reasoned by the following arguments. For small friction coefficients the tangential forces do not contribute significantly to the stability of the packing and hence the packings are not that different from frictionless systems. This behaviour persists, as shown in 1, up to friction coefficients approaching order unity where the typical tangential force first becomes comparable to the normal force. Hence, the friction forces start to play a significant role in stabilising the packing. The precise value of the friction coefficient where this transition occurs is likely to depend on the particle Poisson ratio  $\nu$ . In the work presented here  $\nu = 0$ . Preliminary data with both negative and positive values of  $\nu$  indicate a possible dependence of the critical values on  $\nu$ , but these differences are practically within statistical uncertainty. Other granular simulations [18] with  $\nu = \frac{1}{6}$  find similar behaviour in the packing fraction and coordination number indicating that the data presented here is a general stability property of frictional systems.

Associated changes in the structural properties of the packings with friction are highlighted in 2 and 3, where force network information is presented. 2 shows the normal force networks where the normal forces between particles in contact are represented by lines connecting the centres of the particles. Thicker, darker line shading indicate forces with increasing magnitude. As the critical packing fractions and coordination numbers decrease with increasing friction then density of contacts likewise decreases as is seen in these snapshots. It is also worth pointing out that although the global force network by necessity pervades the system, there is little indication of long-ranged, correlated, force chain structures in the normal forces. 3 shows the distributions of the magnitudes of the normal and tangential forces for packings close to the critical states for different friction coefficients. In all cases, the distributions are characterised by exponential-like tails at larger forces. However, there are some subtle changes occurring at the small force plateau-peak region. Notably, on careful inspection of the data at  $\mu = 0.25$ , which has been emphasised in the figures and corresponds

to a value of the friction coefficient the smallest forces only for friction coefficients where the critical values are decreasing with friction in 1, both the normal and tangential distributions exhibit an upturn at the smallest forces. Thus indicating that the decrease in the critical values indicated in 1 is correlated with the fraction of small forces in the system.

### Scaling

Motivated by earlier studies on frictionless systems, it is possible to rescale all the data for different  $\mu$ , by using the measure  $\Delta\phi \equiv \phi - \phi_c^\mu$ , as the distance for each system for a given  $\mu$ , from their respective jamming transitions, i.e. it is now not appropriate to measure the distance to the jamming transition using just the zero-friction value  $\phi_c^{\mu=0}$ , for different  $\mu$ . 4 shows the power-law scaling, data collapse for the pressure and the excess coordination number  $\Delta z \equiv z - z_c^\mu$ , for all friction coefficients:

$$\begin{aligned} P &\propto \Delta\phi, \\ \Delta z &\propto (\Delta\phi)^{1/2}. \end{aligned} \quad (1)$$

This result shows that jamming frictional spheres look

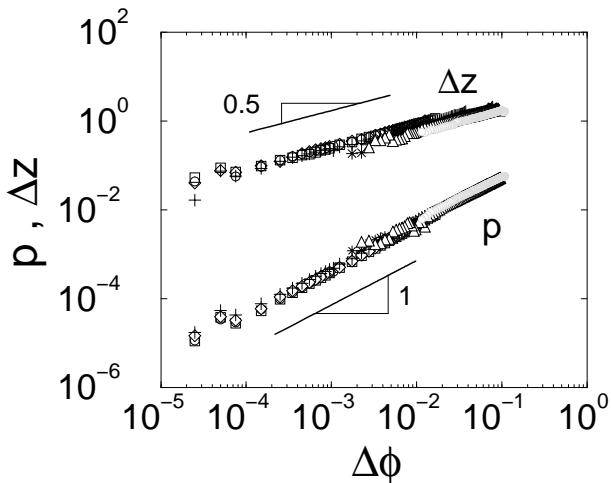


FIG. 4: Power law scaling of the pressure  $p$ , and excess coordination number  $\Delta z$ , as a function of the excess packing fraction,  $\Delta\phi$ , over and above the extrapolated values at the jamming threshold  $\{z_c^\mu, \phi_c^\mu\}$ . Different symbols represent different friction coefficients:  $\mu = 0$  ( $\diamond$ ), 0.001 ( $\circ$ ), 0.01 ( $\square$ ), 0.1 ( $+$ ), 0.5 ( $*$ ), 1 ( $\triangle$ ), and 10 (grey  $\circ$ ). The solid lines represent power laws with exponents 0.5 and 1 as indicated.

like jamming frictionless spheres provided one identifies the friction-specific jamming threshold values  $\phi_c^\mu$  and  $z_c^\mu$ .

Furthermore, the jamming thresholds for the packing fractions and coordination numbers exhibit several power-law relationships as a function of the friction coefficient, as shown in 5 and 6. Up to the large-friction limit, where both  $\phi_c^\mu$  and  $z_c^\mu$  practically saturate, the transition

values relative to the  $\mu = 0$  values, scale as,

$$\begin{aligned} \Delta\phi_{c,0} &\equiv (\phi_c^{\mu=0} - \phi_c^\mu) \sim \mu^{0.74[9]}, \\ \Delta z_{c,0} &\equiv (z_c^{\mu=0} - z_c^\mu) \sim \mu^{0.64[4]}. \end{aligned} \quad (2)$$

The corresponding measures,  $\Delta\phi_{c,\infty} \equiv (\phi_c^\mu - \phi_c^{\mu=\infty})$  and  $\Delta z_{c,\infty} \equiv (z_c^\mu - z_c^{\mu=\infty})$ , relative to the infinite friction limit do not exhibit similar relations, however, the following power laws are also observed:

$$\begin{aligned} \Delta\phi_{c,0} &\sim (\Delta z_{c,0})^{1.23[10]}, \\ \Delta\phi_{c,\infty} &\sim (\Delta z_{c,\infty})^{0.65[8]}, \end{aligned} \quad (3)$$

It is not clear as to the origin of Eq. 2, although the first relation in Eq. 2 is consistent with Eq. 1. These results are similar to two dimensional systems [21], where the corresponding four power law exponents were obtained: 0.77, 0.70, 1.1, and 0.59, and thus hints at some possible underlying universal properties of frictional packings irrespective of dimensionality.

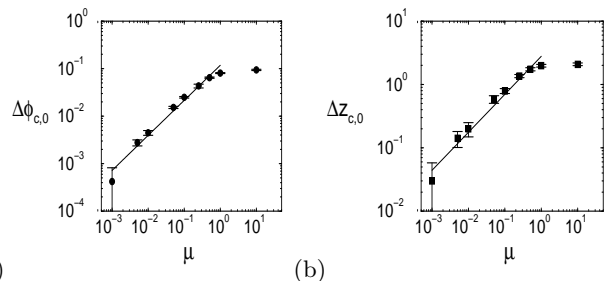


FIG. 5: Power laws for,  $\Delta\phi_{c,0} \equiv (\phi_c^{\mu=0} - \phi_c)$  ( $\bullet$ ), the packing fraction, and  $\Delta z_{c,0} \equiv (z_c^{\mu=0} - z_c)$  ( $\blacksquare$ ), the coordination number, at jamming relative to the zero friction values, over several orders of magnitude in  $\mu$ . Solid lines are power law fits to data described in Eq. 2, with power law exponents  $0.74 \pm 0.09$  and  $0.64 \pm 0.04$  in (a) and (b) respectively.

The results presented thus far have implications regarding the statistical mechanical ensemble formulation of granular (random) packings espoused by Edwards [38]

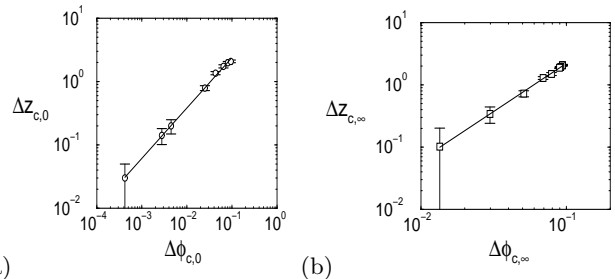


FIG. 6: Power laws between; (a)  $\Delta\phi_{c,0} \equiv (\phi_c^{\mu=0} - \phi_c)$ , and  $\Delta z_{c,0} \equiv (z_c^{\mu=0} - z_c)$ , the jamming values relative to the zero-friction state, and (b)  $\Delta\phi_{c,\infty} \equiv (\phi_c - \phi_c^{\mu=\infty})$  and  $\Delta z_{c,\infty} \equiv (z_c - z_c^{\mu=\infty})$ , the jamming values relative to the large-friction state. Solid lines are power law fits to data described by Eq. 3, with power law exponents  $0.82 \pm 0.06$  and  $1.54 \pm 0.08$  in (a) and (b) respectively.

and has been extensively explored by Makse and co-workers [22] and others [39]. Edwards revision of statistical mechanics proposes that the properties of a granular packing can be computed from a statistical average over equally probable configurations. For infinitely hard and frictional particles the partition function entering the analogue of the canonical ensemble is summed over the full range of all possible states compatible with mechanical stability, from random loose packing,  $\phi_{\text{rlp}} = 0.55$ , up to  $\phi_{\text{rcp}} = 0.64$  [40]. However, the results presented here suggest that generalising to finite friction requires one to take into account friction-dependent constraints: the sum-over-states should only include those mechanically stable states compatible with the value of  $\mu$ , i.e. project onto the sum of states from all possible configurations only the mechanically stable ones [41]. Practically, this may be achieved by cutting-off the sum-over-states at the appropriate value of  $\phi_c^\mu$  [42]:  $\int_{\phi_{\text{rlp}}}^\phi d\phi' \rightarrow \int_{\phi_c^\mu}^\phi d\phi'$ ; or in the microcanonical formalism, states with  $z < z_c^\mu$  should be given zero weight. This is precisely the approach taken by Makse and co-workers who deduced a frictional packing phase diagram [22] which is consistent with the results presented in 1.

### Protocol Dependence

The simulation protocol implemented here generates sphere packings that are statistically identical to other works [6, 19–22], resulting in similar values for the transition packing fraction  $\phi_c^\mu$ , and coordination number  $z_c^\mu$ , as presented in 1 and I. These values correspond to the hard sphere limit where the particles are just touching at the point of jamming. This can be seen by comparing the various interaction and simulation models (linear-spring or Hertzian interaction forces, molecular dynamics or contact dynamics simulations) [18, 20–22, 36]. However, the path taken to arrive at the jamming transition may differ, particularly when friction is present. Because of the hysteretic nature of the frictional forces the precise force configurations explored during this path will depend on the preparation history of the packings.

The major factor influencing the frictional forces are the fraction of slipping contacts  $n_s$ . The plasticity index is defined by [18],  $\zeta \equiv F_t/\mu F_n$ , where  $F_{n,t}$  are the magnitudes of the {normal,tangential} forces. Here, slipping contacts are identified as those contacts at or on the verge of yielding:  $\zeta \geq 0.95$ . The qualitative nature of the results are not sensitive to the precise definition of slipping contacts. The data of 7 shows how the probability distributions  $P(\zeta)$  depend of friction coefficient for packings prepared very close to the jamming threshold. For small friction coefficients  $\mu < 0.2$ , the distributions are dominated by a large fraction of contacts that are close to yielding,  $\zeta > 0.9$ . These systems correspond to points in 1 just before the rapid decrease in  $\phi_c^\mu$  with  $\mu$ . However, for larger friction coefficients,  $\mu > 0.5$ , where the transition values begin to saturate, the weight of the

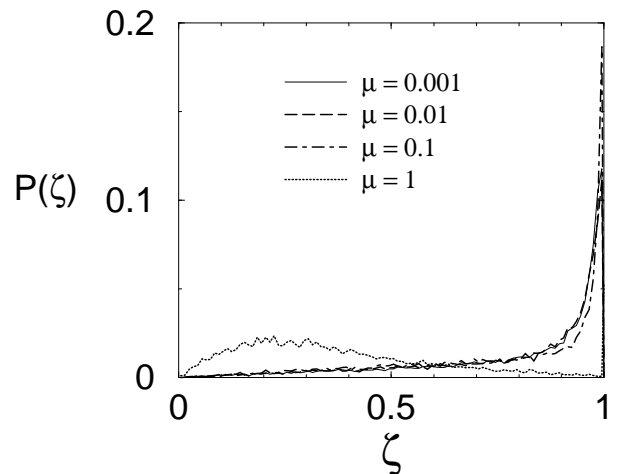


FIG. 7: Distributions,  $P(\zeta)$ , of the plasticity index,  $\zeta \equiv F_t/\mu F_n$ , where  $F_{n,t}$  are the magnitudes of the normal and tangential forces, for different friction coefficients  $\mu$ , within  $10^{-4}$  of the jamming threshold.

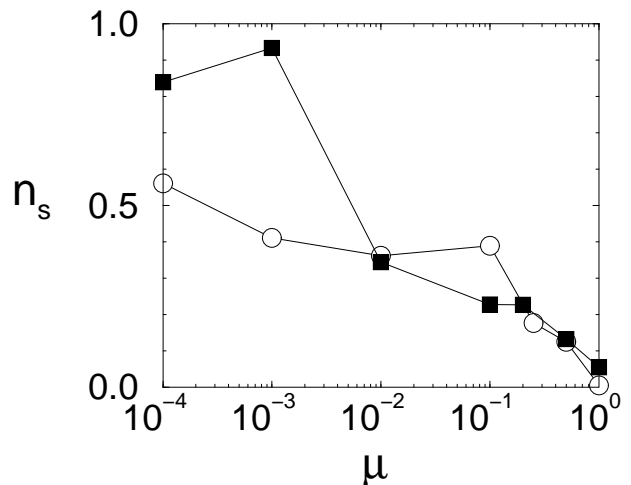


FIG. 8: Fraction of slipping contacts  $n_s$  at  $\Delta\phi(\mu) \approx 10^{-3} - 10^{-4}$  over a large range in friction coefficients. By definition,  $n_s(\mu = 0) = 1$ . The two sets of data represent two slightly different protocols as discussed in the text. Differences at small friction values diminish at larger friction coefficients for the two protocols.

distribution shifts to smaller  $\zeta$ . Hence, a majority of contacts become stabilised as seen by the growth of a hump at  $\zeta \approx 0.25$  for  $\mu = 1$  in 7. Similar changes in  $P(\zeta)$  have been seen in simulations of confined packings [43] and two dimensional systems [21].

Although the qualitative features of the distributions shown in 7 are robust over different protocols, the actual numbers of slipping contacts depends on the preparation history of the packings. To illustrate this point 8 shows the fraction,  $n_s$ , of slipping contacts over a wide range of friction coefficients for packings that are close to the

jamming threshold. The two sets of data correspond to slightly different packing preparation histories. The open symbols are for the protocol used throughout this work to generate the previously shown data: a dilute packing was over-compressed with friction initially set to zero prior to the decompression procedure. The filled symbols, on the other hand, are for packings where friction was set to the desired value during the initial over-compression stage. The differences between the two protocols clearly show up at the lower friction coefficients where the newly modified protocol exhibits a much larger fraction of slipping contacts. The rapid compression with friction leads to a build up of the frictional forces that quickly causes contacts to reach the Coulomb yield criterion as the system is decompressed towards the jamming threshold. However, these differences diminish for larger friction coefficients. The exact nature of the frictional build up and relaxation is currently under investigation. It is also worth pointing out that the extrapolated jamming thresholds are identical within statistical uncertainty between the two protocols. Thus, the protocol dependence does not seem to affect the geometrical properties of the packing, but will likely have an effect on mechanical properties, such as yielding under flow or the application of external forces.

To probe the nature of protocol dependence further, the algorithm used to generate the packings was also modified in the following ways: In one case a dynamic friction model was used that depends only on the instantaneous friction force. For this system the jamming threshold lies much closer to the frictionless limit. In the other data, the history of the contacts was reset at different intervals during the simulation procedure thereby suppressing the build-up of frictional forces. The corresponding evolution of the coordination number with packing fraction is shown in 9 for packings these packings where the contact history and frictional forces were treated differently.

Thus, erasing the history of the frictional forces between particles in contact can have a profound effect on the resulting evolution of the packing. What 9 demonstrates is that friction strongly influences the jamming thresholds and hence the possible range of mechanically stable states for a given friction coefficient. This may therefore explain, in part, the observation why real, frictional granular materials, more often than not, tend to form packings that are intermediate between the random close and random loose limits: even minor rearrangements that cause the particles to momentarily come out of contact will erase the history of frictional contacts and thus the system will appear to be composed of particles of a lower friction coefficient than their actual values. This aspect of the history dependence of the frictional forces has been utilised recently in experiments on real, frictional, granular particles made to mimic frictionless systems [44].

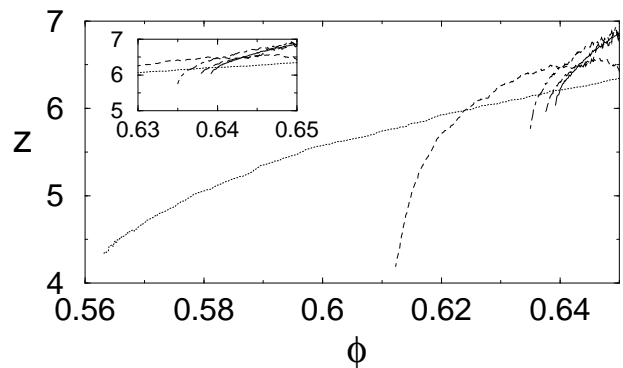


FIG. 9: Evolution of the coordination number,  $z$ , with decreasing packing fraction,  $\phi$ . Line styles represent different friction models: frictionless ( $\mu = 0$ , solid line); history-dependent static friction model (dotted), static-friction model reset at different rates (dot-dash and dash), and dynamic instantaneous friction model with no contact history (long-dash),  $\mu = 1.0$ . Inset shows the random close packing region.

## Conclusions

In summary, cohesionless, frictional spheres that interact only on contact, exhibit a jamming transition that shares many similarities with that for frictionless systems, provided one identifies the appropriate friction-dependent jamming transition packing fraction  $\phi_c^\mu$ , and coordination number  $z_c^\mu$ . Using these friction-dependent quantities rather than just the frictionless and frictional isostatic values may lead to a better understanding of existing scaling results [30, 45]. In saying that, the role of packing generation protocol and friction-induced history dependence persists as a topic that has received relatively little attention to date. Understanding how packings traverse the packing stability diagram of 1 will likely help resolve some of these issues.

Random loose packing,  $\phi_{rlp} \approx 0.55$ , appears to be a state that can only be achieved in the large-friction limit. These results, however, do not preclude the fact that even lower values of  $\phi_{rlp}$  may be obtained using different protocols, such as sedimenting particles in a fluid [46], or tuning the particle interactions to include additional forces, such as cohesion [47, 48].

The power-law dependence on  $\mu$  of both  $\phi_c$  and  $z_c$ , relative to the frictionless system hints at a more universal behaviour. The origin of these scalings remain unclear although one possible explanation for the results of 5 and 6 might lie in spatial correlations between the frictional forces. As shown in 8, there is a systematic decrease in the fraction of slipping contacts with increasing friction. One might therefore expect that for small friction coefficients there are large spatial regions of contacts that are slipping, whereas for large friction, these are replaced by non-mobilised contacts. Hence, fluctuations are small in either case. However, intermediate between these two extreme states, large-scale, fluctuating regions might oc-

cur. Preliminary data suggests that there is indeed an increase in correlations that follow these arguments and such ideas are currently being pursued.

Applications of the results presented here could potentially pave the way towards a generalised formulation of an equation of state for granular materials. Progress along these lines has been made recently [22]. However, the hysteretic nature of the frictional forces can have a significant effect on the properties of the packing. It is interesting to note that the friction coefficients of many materials lie in the range  $0.01 \leq \mu \leq 1$ . Coincidentally, these values of  $\mu$  correspond to the region of mechanically stable states where small changes in  $\mu$  can lead to large changes in the packing fraction and coordination number of the packing. Hence, any processes that cause changes in the surface friction of the constituent

particles, such as roughening or polishing, can result in packings with dramatically different stability properties. Alternatively, materials could be designed with varying mechanical properties based on their frictional properties.

### Acknowledgements

It is a pleasure to thank M. van Hecke and M. Schröter for several insightful discussions related to this work. Support from an SIU ORDA faculty seed grant and the National Science Foundation CBET-0828359 is greatly appreciated.

- 
- [1] J. D. Bernal and J. Mason, *Nature*, 1960, **188**, 910.  
 [2] G. D. Scott, *Nature*, 1960, **188**, 908.  
 [3] J. G. Berryman, *Phys. Rev. A*, 1983, **27**, 1053.  
 [4] S. Torquato, T. M. Truskett and P. G. Debenedetti, *Phys. Rev. Lett.*, 2000, **84**, 2064.  
 [5] H. A. Makse, D. L. Johnson and L. M. Schwartz, *Phys. Rev. Lett.*, 2000, **84**, 4160.  
 [6] C. S. O'Hern, L. E. Silbert, A. J. Liu and S. R. Nagel, *Phys. Rev. E*, 2003, **68**, 011306.  
 [7] A. Donev, S. Torquato and F. H. Stillinger, *Phys. Rev. E*, 2005, **71**, 011105.  
 [8] L. E. Silbert, A. J. Liu and S. R. Nagel, *Phys. Rev. E*, 2006, **73**, 041304.  
 [9] R. D. Kamien and A. J. Liu, *Phys. Rev. Lett.*, 2007, **99**, 155501.  
 [10] G. Y. Onoda and E. G. Liniger, *Phys. Rev. Lett.*, 1990, **64**, 2727.  
 [11] M. Jerkins, M. Schröter, H. L. Swinney, T. J. Senden, M. Saadatfar and T. Aste, *Phys. Rev. Lett.*, 2008, **101**, 018301.  
 [12] *Jamming and Rheology*, ed. A. J. Liu and S. R. Nagel, Francis & Taylor, New York, 1999.  
 [13] *Unifying Concepts in Granular Media and Glasses*, ed. A. Coniglio, A. Fierro, H. J. Herrmann and M. Nicodemi, Elsevier, Amsterdam, 2004.  
 [14] C. S. O'Hern, S. A. Langer, A. J. Liu and S. R. Nagel, *Phys. Rev. Lett.*, 2002, **88**, 075507.  
 [15] S. Alexander, *Phys. Rep.*, 1998, **296**, 65.  
 [16] C. F. Moukarzel, *Phys. Rev. Lett.*, 1998, **81**, 1634.  
 [17] J.-N. Roux, *Phys. Rev. E*, 2000, **61**, 6802.  
 [18] L. E. Silbert, D. Ertas, G. S. Grest, T. C. Halsey and D. Levine, *Phys. Rev. E*, 2002, **65**, 031304.  
 [19] H. P. Zhang and H. A. Makse, *Phys. Rev. E*, 2005, **72**, 011301.  
 [20] T. Unger, J. Kertész and D. E. Wolf, *Phys. Rev. Lett.*, 2005, **94**, 178001.  
 [21] K. Shundyak, M. van Hecke and W. van Saarloos, *Phys. Rev. E*, 2007, **75**, 010301(R).  
 [22] C. Song, P. Wang and H. A. Makse, *Nature*, 2008, **453**, 629.  
 [23] S. F. Edwards, *Philos. Mag. B*, 1998, **77**, 1293.  
 [24] L. F. Liu, Z. P. Zhang and A. B. Yu, *Physica A*, 1999, **268**, 433.  
 [25] L. E. Silbert, G. S. Grest and J. W. Landry, *Phys. Rev. E*, 2002, **66**, 061303.  
 [26] T. Aste, *J. Phys.:Condens. Matter*, 2005, **17**, S2361.  
 [27] A. R. Abate and D. J. Durian, *Phys. Rev. E*, 2006, **74**, 031308.  
 [28] T. S. Majmudar, M. Sperl, S. Luding and R. P. Behringer, *Phys. Rev. Lett.*, 2007, **98**, 058001.  
 [29] N. Mitarai and H. Nakanishi, *J. Phys. Soc. Jpn.*, 2001, **70**, 2809.  
 [30] E. Somfai, M. van Hecke, W. G. Ellenbroek, K. Shundyak and W. van Saarloos, *Phys. Rev. E*, 2007, **75**, 020301(R).  
 [31] P. A. Cundall and O. D. L. Strack, *Géotechnique*, 1979, **29**, 47.  
 [32] O. R. Walton and R. L. Braun, *J. Rheol.*, 1986, **30**, 949.  
 [33] *Experimental and Computational Techniques in Soft Condensed Matter Physics*, ed. J. Olafsen, Cambridge University Press, Cambridge, 2010, ch. 5.  
 [34] L. Rothenburg, A. A. Berlin and R. J. Bathurst, *Nature*, 1991, **354**, 470.  
 [35] D. J. Durian, *Phys. Rev. E*, 1997, **55**, 1739.  
 [36] I. Agnolin and J.-N. Roux, *Phys. Rev. E*, 2007, **76**, 061302.  
 [37] L. Rothenburg and N. P. Kruyt, *International Journal of Solids and Structures*, 2004, **41**, 5763.  
 [38] S. F. Edwards and R. B. S. Oakeshott, *Physica A*, 1989, **157**, 1080.  
 [39] S. Henkes and B. Chakraborty, *Phys. Rev. E*, 2009, **79**, 061301.  
 [40] E. R. Nowak, J. B. Knight, E. Ben-Naim, H. M. Jaeger and S. R. Nagel, *Phys. Rev. E*, 1998, **57**, 1971.  
 [41] P. Richard, M. Nicodemi, R. Delannay, P. Ribière and D. Bideau, *Nature Materials*, 2005, **4**, 121.  
 [42] M. Schröter, D. I. Goldman and H. L. Swinney, *Phys. Rev. E*, 2005, **71**, 030301(R).  
 [43] J. W. Landry, G. S. Grest, L. E. Silbert and S. J. Plimpton, *Phys. Rev. E*, 2003, **67**, 041303.  
 [44] G.-J. Gao, J. Blawdziewicz, C. S. O'Hern and M. Shattuck, *Phys. Rev. E*, 2009, **80**, 061304.  
 [45] V. Magnanimo, L. La Ragione, J. T. Jenkins, P. Wang and H. A. Makse, *Europhys. Lett.*, 2008, **81**, 34006.  
 [46] G. Farrell, K. M. Martini and N. Menon, unpublished.

- [47] K. J. Dong, R. Y. Yang, R. P. Zou and A. B. Yu, Phys. Rev. Lett., 2006, **96**, 145505.
- [48] G. Lois, J. Bławdziewicz and C. S. O'Hern, Phys. Rev. Lett., 2008, **100**, 028001.